Catalysis Letters 20 (1993) 59–71

A multiple-scattering approach to the study of X-ray absorption spectra of anatase and rutile

F. Bohr, M.F. Ruiz-López

Laboratoire de Chimie Theorique, UA CNRS 510, Umiversité de Nancy I,
BP 239, 54506 Vandoeuvre les Nancy, France

and

A. Muñoz-Páez [1]

Departamento de Química Inorgánica and Instituto de Ciencia de Materiales
(Universidad de Sevilla-CSIC), Apdo. 553, 41071 Sevilla, Spain

Theoretical computations of the X-ray absorption spectra of the crystalline forms of TiO_2, rutile and anatase, have been carried out in order to analyze the influence of multiple scattering contributions to the absorption coefficient. The cluster size used in the computations after making a detailed study of shell contributions, has been 75 atoms for rutile and 63 for anatase. This work has been envisaged as a suitable starting point to the analysis of experimental data for the more complicated TiO_2 amorphous systems involved in catalytic processes.

Keywords: EXAFS; XANES; TiO_2; multiple scattering

1. Introduction

Titania catalyzes several photo-assisted processes, like partial oxidation of hydrocarbons, decomposition of water (to form H_2 and O_2) and reduction of NH_3 due to its semiconducting oxide character [1]. The acid–base properties of its surface make it active in alcohol decomposition. In addition, it has been widely used as a support in metal catalysts due to its surface and bulk properties and to its ability to increase the activity and selectivity of the metal in hydrogenation and dehydrogenation processes [2]. When acting as a catalyst or support, this oxide is in most cases in the crystalline forms of anatase or rutile. Nevertheless, there is an increasing interest in amorphous TiO_2 based systems where titanium oxide is deposited or embedded in a matrix of a second oxide to increase the surface area and thus catalytic selectivity and/or activity. These mixed compounds have additional interest in the field of material science to prepare titania glasses and ceramics [3].

---

[1] To whom correspondence should be addressed.

Since these systems do not show long-range order, X-ray absorption spectroscopies, both EXAFS and XANES are the best ways of obtaining information about geometric structure. According to the interest of these new amorphous materials, the XANES region of the Ti K-edge of crystalline and amorphous oxides, alcoholates and chlorides, have been the subject of several theoretical and experimental studies [4–10], although a final interpretation has not been reached. For instance, Emili et al. [4] have related the pre-edge of Ti with the coordination geometry around Ti centers, in TiO_2–SiO_2 glasses, while Asbrink et al. [5] have related the same feature to oxidation state in TiO_2–VO_x systems. On the other hand, Grunes [6] has assigned the features of the anatase and rutile edges on the basis of calculations for TiO_6 octahedra, but these units do not reproduce the periodicity and the long-range order present in the crystalline structures. In the more complete work by Brydson et al. [7], the XANES spectrum for a system with several atomic shells has been computed using a multiple-scattering formalism.

EXAFS data have also been reported in the literature for anatase [11,12] and other amorphous titanium compounds [9,10]. In the case of anatase, it has been shown that, whenever a multiple shell fit is carried out, correlation to within 0.1 Å of atomic position is lost beyond distances involving more than three octahedra coupling [11].

All these studies reveal the importance of titanium oxides and titanium based systems, as well as the difficulties in interpreting their X-ray absorption spectra, nearly the only tool to obtain information about coordination geometries in amorphous systems. Then the thorough analysis of the spectra of the crystalline oxides, having a well known structure, appears to be an important step in the understanding of these amorphous systems.

There is a general agreement that multiple-scattering (MS) approaches have to be used in the quantitative reproduction of the XANES region. On the other hand, for the analysis of the EXAFS region, the plane wave, single-scattering (SS) approximation is currently used [13]. However, MS effects are well known in the case of linear systems [14]. Additional references dealing with the particular problems appearing when using EXAFS and XANES in the field of catalysis are those of Lytle and Horsley [15]. In other cases it is gaining supporters [16] of the idea that the curved wave multiple scattering theory can provide a unified approach for the X-ray absorption spectra, including both, the extended and the near edge regimes [17,18]. Important aspects that have to be studied carefully when using this theory are the enumeration of MS paths, the shadowing effects in linear paths, the order to be considered in MS contributions, the cluster sizes and the energy ranges. For a recent review on the MS theory on XAS see for instance [19].

In this paper, we present detailed theoretical computations for the crystalline titanium oxides rutile and anatase based on the local density approximation and using MS approach. The XANES region has been already analyzed in detail in a previous publication [20] but, for completeness, we include here the most important results obtained.

2. Experimental

XAS experiments were performed on the EXAFS station 8.1 in the Synchrotron Radiation Source at Daresbury Laboratories with ring energies of 2 GeV and ring currents of 250 MA. The EXAFS spectrum was recorded at −198°C in an in situ cell [21], where the sample was placed after being pressed with BN into a wafer with an absorbance (μx) of 2.5 at the titanium K-edge, ensuring an optimum signal/noise ratio.

Crystalline TiO_2 anatase was used as supplied by British Titan Products (Billingham, UK). Rutile was prepared by hydrolysis of $TiCl_4$ (from the same suppliers) followed by calcination at 540°C for 2.5 h. The crystallinity of both samples was determined by X-ray diffraction.

3. Computations

The spectra have been computed using the local density approximation. Muffin-tin type potentials estimated by an average sum of atomic potentials have been used. Though this is a crude approximation, previous work has shown that it gives good results in highly symmetric systems such as those studied here. The muffin-tin radii used in this work were obtained according to the Norman criterion so that the atomic spheres are almost tangent: this gives $R_{\mathrm{Ti}} = 2.04$ a.u. and $R_{\mathrm{O}} = 1.66$ a.u.

Theoretical spectra are also quite sensitive to the type of the local density approximation for the exchange-correlation potential. In this work we use the energy dependent Dirac–Hara exchange potential [22] which seems to give the best results in XAS studies [23,24]. The spectra are then convoluted to account for inelastic losses using the Hedin–Lundqvist [25] approach which permits calculation of the effective mean-free path of the photoelectron at a given kinetic energy. The Fermi level and the interstitial potential have been estimated as previously proposed [20].

It should be pointed out that in the computation of the EXAFS spectra, it is useful to expand the total absorption coefficient in a power series as

$$\sigma = \sigma_0 \Sigma_{i,j,k}^{\mathrm{atoms}} (1 + \chi_2^{oio} + \chi_3^{oijo} + \chi_4^{oijko} + \ldots)$$

where σ_0 is the pure atomic absorption coefficient of the ionized species and $\chi_n^{oijk\ldots o}$ may be interpreted as the contribution due to all processes in which the electron is scattered $n-1$ times. In this formula, o represents the absorbing atom and $i, j, \ldots$ the scattering atoms. Thus, χ_2^{oio} represents the single-scattering (SS) o–i–o path contribution, χ_3^{oijo} the double scattering o–i–j–o path contribution and so forth. Detailed formulae may be found elsewhere [16,17].

Computations have been made using the program by Natoli and Benfatto [17] for the edge spectra, and MSXAS program [26] for the scattering path contributions in the EXAFS region.

Additional data analysis of the EXAFS spectrum of anatase using single scattering approach [27] has been carried out. Curve fitting has been done in *k* and *R* space using phase shift and backscattering amplitude functions obtained from experimental spectra.

4. Results and discussion

4.1. DESCRIPTION OF THE MODELS

In rutile and anatase six oxygen atoms are placed around Ti atoms forming slightly distorted octahedra and every oxygen atom is between three titanium atoms. They are both tetragonal and the main structural differences lie in the way the octahedra are deformed and linked together [28]. In our computations we shall consider clusters of atoms consisting of one Ti atom (the absorbing atom) surrounded by a given number of neighboring atoms (either O or Ti) for which the distance with respect to the central Ti atom is shorter than a given value. The basic unit is a deformed octahedron with two different Ti–O distances. In rutile there are four Ti–O distances at 1.946 Å and two at 1.984 Å. The symmetry group is D_{2h}. In anatase, the corresponding distances are 1.937 and 1.964 Å and the symmetry group is D_{2d}.

The computation of the XAS spectra of a crystalline solid requires the choice of a convenient model representing the electronic properties of the solid as well as possible. Owing to computational limitations the number of atoms considered should not be very large, but keeping this number too small could lead to inaccurate or even unrealistic results. So we have regarded detailed analysis of the effect of cluster size on computations as crucial.

4.2. XANES

Fig. 1 compares the results obtained for the K-edge spectrum of several models of rutile with increasing number of atomic shells. All these computations have been performed using the simple Xα potential. Descriptions of the models are summarized in table 1. In the simplest model 1 we have the basic octahedron formed by one Ti atom surrounded by six oxygen atoms. In other models an increasing number of shells formed by Ti and O atoms have been added. The computation for the model including a total number of 105 atoms did not change the results of the 75 atoms model appreciably and is not included in the figure. From these results one concludes that at least 51 atoms (model 3) should be included in the computations in order to get all the spectral features, whose intensity, however, may still be modified by further shells. A good convergence is obtained for model 4 (75 atoms). This model includes all atoms lying in a radius of 5.5 Å and may be considered as the simplest cluster which correctly describes the electronic properties of the solid.

The computed absorption coefficient is compared with experimental data in

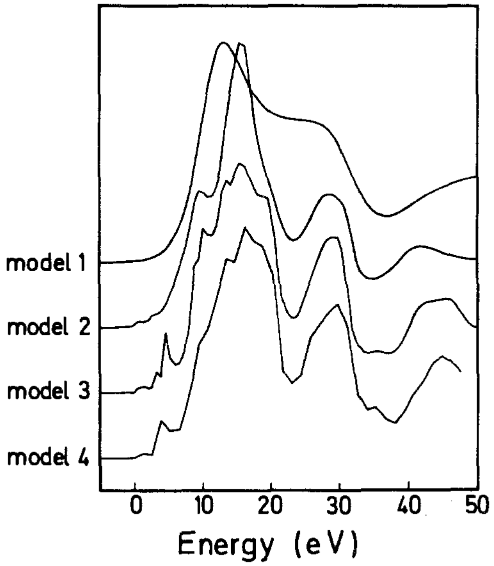

Fig. 1. Computed XANES spectra (arbitrary scale) for model systems of rutile with different dimension: (1) model 1 (TiO_6), (2) model 2 ($Ti_{11}O_{14}$), (3) model 3 ($Ti_{15}O_{36}$) and (4) model 4 ($Ti_{31}O_{44}$).

fig. 2. We now use the more elaborate Dirac–Hara exchange potential. Most of the experimental peaks are correctly predicted by the computations: the relative intensities for the three pre-edge features A_1, A_2, A_3, the edge feature B and the resonances D and E are computed reasonably well. For features C_1 and C_2 the agreement is not so good but our results require some comments. In the computed spectrum of fig. 2, only one peak (C) seems to be present while in the experimental spectrum two peaks (C_1 and C_2) are clearly observable. A detailed analysis of the computations [16] shows a shoulder in the computed spectrum between (B) and (C) corresponding to a shoulder in the b_{2u} symmetry component. In the Xα computation (see fig. 1), this gives a flat maximum in the spectrum that the Hedin–Lundqvist convolution tends to erase. Thus, the theoretical model predicts

Table 1
Models for crystalline TiO_2 rutile

Model	No. of atoms		No. of shells	Radius[a] (Å)
	Ti	O		
1	1	6	1	1.983
2	11	14	3	3.569
3	15	36	5	4.615
4	31	44	7	5.500
5	37	68	9	6.495

[a] Distance from the absorbing Ti atom to the most distant atom.

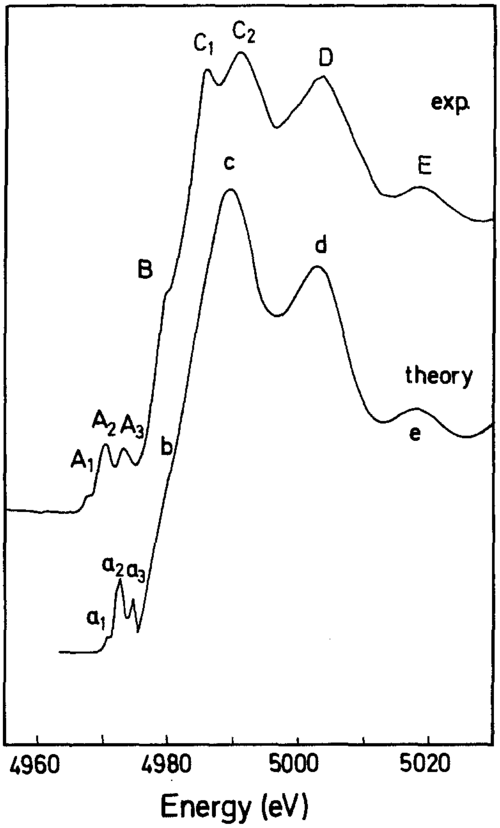

Fig. 2. Comparison between the experimental spectra of rutile (top) and the computed spectra using model 4 and Dirac–Hara potential (bottom). The spectra are plotted in an arbitrary scale but the theoretical curve has been normalized so that the intensity of peak C is equal to that of the experimental curve.

two features in this region, in agreement with experiment, but the computations fail to reproduce the energy separation and the relative intensities correctly.

The computed spectrum for anatase is compared to experimental data in fig. 3. The model used for anatase is comparable to that used for rutile, i.e., all atoms within a sphere of radius 5.5 Å around the absorbing Ti atom are included; this gives a cluster of 63 atoms ($Ti_{29}O_{34}$).

The spectra of anatase and rutile present substantial differences which reflect their different long-range order. Most of the remarks made for rutile also stand for anatase. Notice that, again, a single peak (C) is predicted. Feature (D) is computed at a lower energy than the corresponding peak in rutile, in agreement with experimental data although the experimental spectrum has more than a single structure. The resonance labeled E in rutile is not present in anatase but a weak signal is observed at about 5017 eV in the experimental spectrum of anatase.

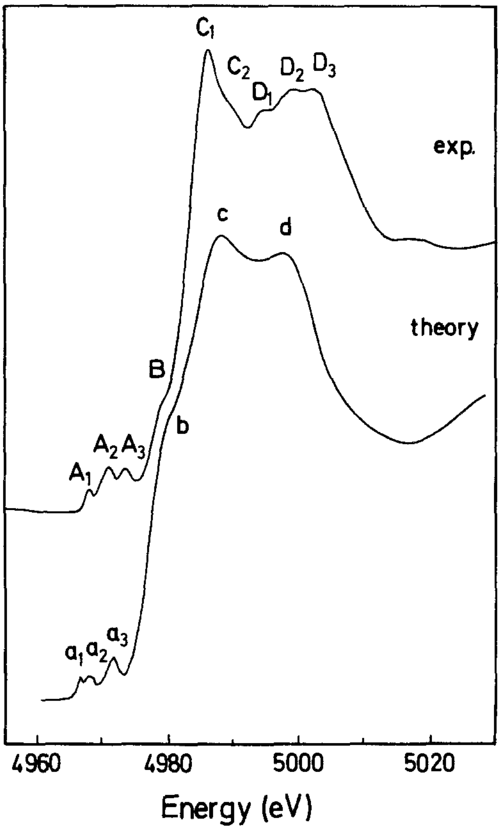

Fig. 3. Comparison between the experimental spectra of anatase (top) and the computed spectra using a model equivalent to model 4 in rutile (bottom). The Dirac–Hara potential is used. The spectra are plotted in an arbitrary scale but the theoretical curve has been normalized so that the intensity of peak C is equal to that of the experimental curve.

In relation with the pre-edge features, an object of controversy in the literature [4–8], it has to be pointed out that they are very sensitive to the number of atoms considered in the model. Restricted MO calculations [16] discard quadrupole transition as the origin of these features, and show that these features are very sensitive to Ti–Ti distances.

4.3. EXAFS

In the computation of the EXAFS spectra of anatase and rutile the most significant scattering paths have been chosen in each case, and their contribution to the absorption coefficient calculated. The same computational details operate here.

The scattering paths considered in the case of anatase are those with total length less than 10 Å. This includes only the terms χ_2, χ_3, χ_4 of the scattering series since no χ_n with $n > 4$ were found for scattering paths < 10 Å. In fig. 4, we compare single

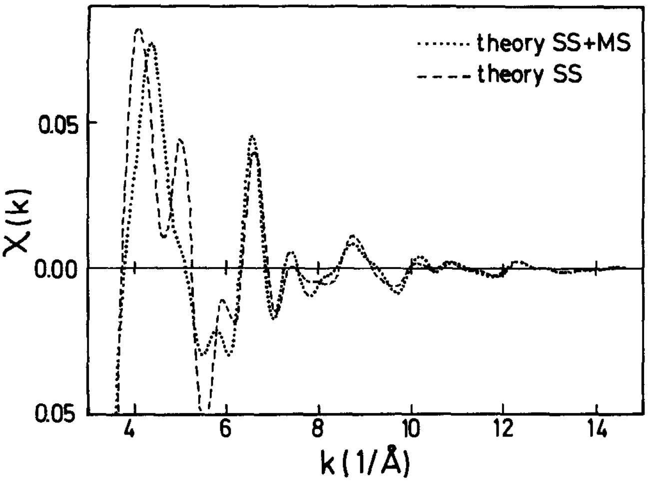

Fig. 4. Relative amplitudes of the calculated EXAFS oscillations for the single and multiple scattering signals in the case of anatase: (- - -) calculated contribution of the SS path, (· · ·) the sum of SS + MS contribution. See text for details of the scattering paths included.

scattering calculations versus multiple scattering + single scattering calculations. Note that the introduction of multiple scattering effects basically induces changes in the low energy region of the spectrum, i.e. between 4 and 6 $Å^{-1}$, the rest of the single scattering curve remaining unchanged. Thus, MS effects do not produce drastic changes in the spectrum. According to this, a standard SS calculation [27] using six shells from Ti–O and Ti–Ti contributions reproduces quite well the Fourier filtered data, as shown in fig. 5 (see structural parameters in table 2). The main problem in this fit comes from the contributions of shells 3, Ti–O, and 4, Ti–Ti, nearly at the same distance and opposite in phase.

In contrast with the results for the spectrum of anatase, the EXAFS spectrum of rutile could not be reproduced using SS routines. From this fact we inferred that MS contributions should be significant in this case, as suggested also by the comparative plot included in fig. 6, which shows considerable differences between SS calculations and experimental signal. As a first approach, MS calculations similar to those performed in the case of anatase were carried out, although in this case χ_2, χ_3, χ_4, χ_5, χ_6 terms of the scattering series for path lengths < 12 Å were calculated. As shown in fig. 7, the agreement between experiment and calculations improves only very slightly when this type of MS contributions is taken into account.

In order to evaluate the contribution of higher order scattering terms, in a following step we carried out a full computation of the total absorption coefficient similar to that made in the XANES region, i.e. by direct matrix inversion. For computational restrictions, the value of k was kept below 7 $Å^{-1}$. The cluster for this calculation was the 75 atoms cluster ($2R = 11$ Å), the minimum cluster size

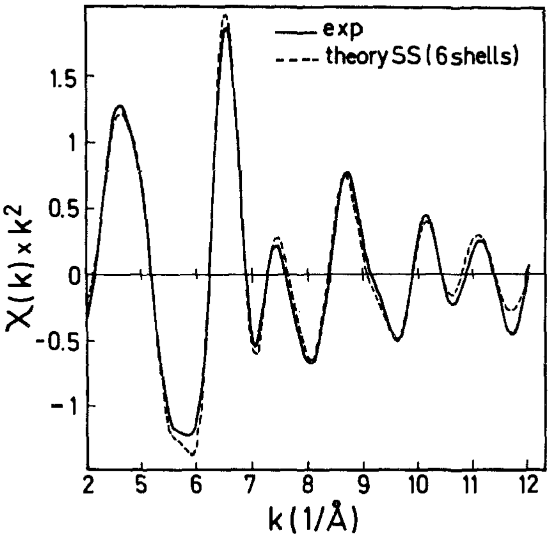

Fig. 5. Comparison of experimental and calculated EXAFS oscillations for anatase: (—) the Fourier filtered ($\Delta k = 2.7$–12.5 Å^{-1}, $\Delta R = 0.9$–4.7 Å) experimental spectrum, (- - -) calculated contribution $\chi_2(E)$ of the SS path (six shells).

necessary to reproduce experimental data at low energy. Moreover, a cluster of 105 atoms ($2R < 13$ Å) was also considered. The results show that the absorption coefficient in the EXAFS region is almost identical for these two clusters, as was already the case in the XANES. Nevertheless the assumption that MS effects

Table 2
EXAFS fitted parameters and crystallographic data for anatase

Shell	EXAFS parameters			Crystallographic data	
	N[a]	R[b] (Å)	$\Delta\sigma^2$[c] (Å^2)	$N \times R$ (Å)	octahedron
Ti–O	6.6	1.94	0.00367	4 × 1.93	1st
Ti–Ti	3.8	3.06	−0.00469	4 × 3.04	2nd
Ti–O	12.2	3.81	0.00080	8 × 3.86	
Ti–Ti	4.2	3.84	−0.00194	4 × 3.78	
Ti–O	13.4	4.28	0.00150	8 × 4.25	3rd
				8 × 4.27	
				4 × 4.75	
Ti–Ti	8.5	4.87	0.00131	8 × 4.85	4th

[a] Coordination number.
[b] Coordination distances.
[c] Deye–Waller factor.

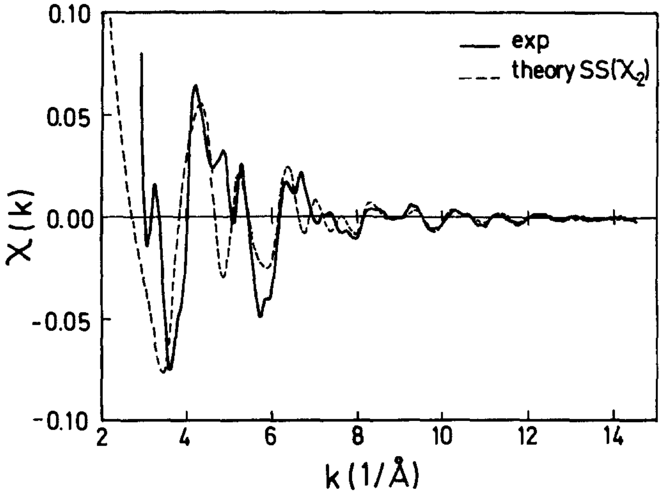

Fig. 6. Comparison of experimental and calculated EXAFS oscillations for rutile: (—) the experimental spectrum, (- - -) calculated contribution $\chi_2(E)$ of the SS path.

should be relevant in this compound, i.e. that the terms higher than χ_2 in the scattering series should give a significant contribution to the EXAFS spectrum, has been shown to be well addressed. This can be clearly appreciated in fig. 8, where the terms of the scattering series have been plotted independently, which shows that the intensity of terms of order > 5 is not negligible for the studied range of energy. Finally, it should be pointed out that some scattering paths connecting atoms which are not included in these clusters could lead to noticeable MS contributions

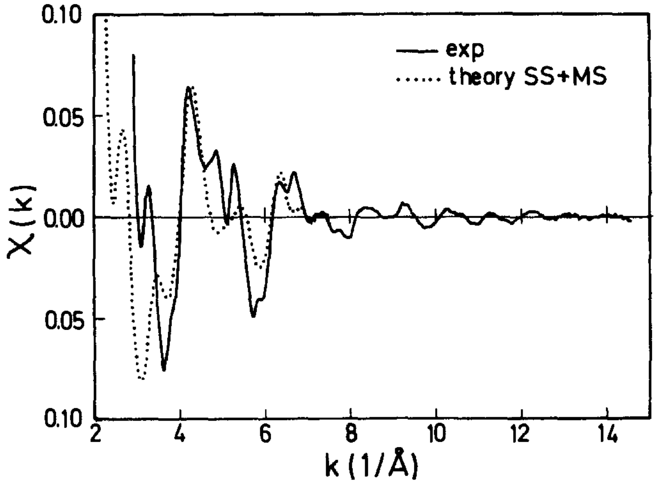

Fig. 7. Comparison of experimental and calculated EXAFS oscillations for rutile: (—) the experimental spectrum, (...) sum of the calculated contributions SS (χ_2) and MS ($\chi_3, \chi_4\chi_5\chi_6, R \leqslant 12$ Å).

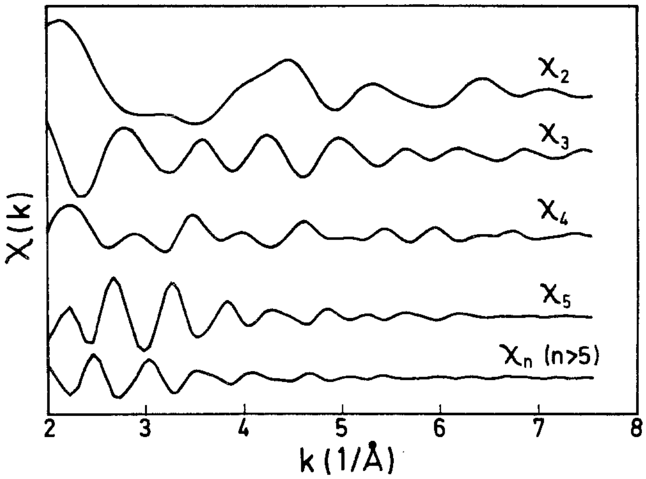

Fig. 8. Terms of the scattering series calculated by direct matrix inversion for a 75 atoms cluster of rutile.

because of the special structure of rutile. Indeed, the Ti atoms of the octahedra sharing corner and edges are perfectly aligned in four directions, one along the diagonal of the unit cell and the three others along perpendicular axes to the center of the faces. Due to this alignment, the shadowing effect can enhance the intensity of the higher terms in the scattering series even for path lengths superior to 12 Å. Thus, in a further effort to reproduce the experimental spectrum we have included all scattering paths in these directions up to $R = 18$ Å and scattering order $n = 6$ and their contribution was added to that obtained for the 75 atoms cluster. As can be seen in fig. 9, some improvement is achieved by this extension of the calculation although the results obtained are still far from satisfactory reproductions of experimental data.

The poor agreement between experiment and computations could point to the inability of one-electron theories to reproduce the EXAFS spectrum of rutile, since the type of calculations and the cluster size are appropriate for this type of systems.

5. Conclusions

MS effects have been shown to give significant contributions to the X-ray absorption spectra of rutile and anatase. Though some differences between experimental and computed XANES have been observed, most of the features are well reproduced by the theory. In the EXAFS region, the spectrum of anatase is well reproduced by SS approach above 6 $Å^{-1}$. Conversely, in the case of rutile, the best computations carried out in our work, which approaches the limit of what can be obtained using a one-electron theory in the MS formalism, still presents substantial

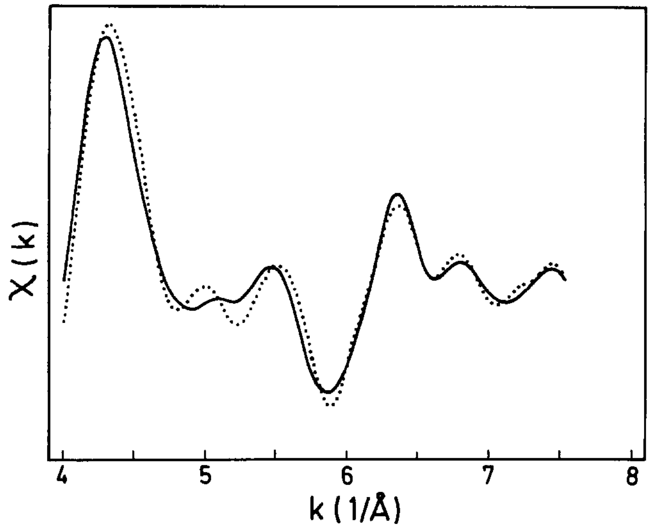

Fig. 9. Effect of the very long linear paths on the rutile spectrum: (—) full computations for the 75 atoms cluster, (···) full computations connected by linear path contributions up to 18 Å.

differences with experimental data. The main limitations of the present computations are the use of a muffin-tin model potential and the neglect of many-body interactions. The former is not expected to have a great effect on our results since the systems studied are quite symmetrical and non-spherical corrections to the molecular potential should be small. The influence of the second is difficult to predict but it is probably larger. Further work is required to evaluate many-body effects on the X-ray absorption spectra of these systems. Moreover, the role played by geometrical factors should be examined in order to explain the results obtained in this work for anatase and rutile which illustrate, anyway, the complexity of a quantitative analysis of experimental EXAFS data for TiO_2 crystalline compounds.

Acknowledgement

The authors wish to thank C.R. Natoli for making available some of the software used in this work. They also thank the Spanish DGICYT (project number PB 89-642) for financial support and the SRS (Daresbury Laboratory, SERC, UK) for allocation of beamtime and help during XAS measurements.

References

[1] H. Kung, in: *Transition Metal Oxides*, Studies in Surface Science and Catalysis, Vol. 45, eds. B. Delmon and J.T. Yates, (Elsevier, Amsterdam, 1989) chs. 10, 14.
[2] K. Foger, Catal. Sci. Technol. 6 (1984) 227.
[3] H.D. Gesser and P.C. Goswami, Chem. Rev. 89 (1989) 765.

[4] M. Emili, L. Incoccia, S. Mobilio, G. Fagherazzi and M. Guglielmi, J. Non-Cryst. Solids 74 (1985) 129.
[5] S. Asbrink, G.N. Greaves, P.H. Hatton and K. Garg, J. Appl. Cryst. 19 (1986) 331.
[6] L.A. Grunes, Phys. Rev. B 27 (1983) 2111.
[7] R. Brydson, H. Sauer, W. Engel, J.M. Thomas, E. Zeitler, N. Kosugi and H. Kuroda, J. Phys.: Condens. Matter 1 (1989) 797.
[8] B. Poumellec, R. Cortes, G. Tourillon and J. Berthon, in: *2nd European Conf. on Progress on X-ray Synchro. Rad. Res.*, Conf. Proc. Vol. 25, eds. A. Balerna, E. Bernieri and S. Mobilio (SIF, Bologna, 1990) p. 23.
[9] F. Babonneau, S. Doeuff, A. Leaustic, C. Sanchez, C. Cartier and M. Verdaguer, Inorg. Chem. 27 (1988) 3166.
[10] A. Muñoz-Paez and G. Munuera, in: *Preparation of Catalyst V*, Studies in Surface Science and Catalysis, Vol. 62, eds. G. Poncelet, P.A. Jacobs, P. Grange and B. Delmon (Elsevier, Amsterdam, 1991) p. 627.
[11] R. Kozlowski, R.F. Pettifer and J.M. Thomas, J. Phys. Chem. 87 (1983) 5172.
[12] G. Vlaic, J.C.J. Bart, W. Cavigiolo, S. Mobilio and G. Novarra, A. Natuurforsch. 36a (1981) 1192.
[13] P.A. Lee and J.B. Pendry, Phys. Rev. B 11 (1975) 2795;
B.K. Teo, J. Am. Chem. Soc. 103 (1981) 3990;
J.J. Boland, S.E. Crane and J.D. Baldeswieler, J. Chem. Phys. 77 (1982) 142;
S.J. Gurman, N. Binsted and I. Ross, J. Phys. C 19 (1986) 1845;
S.P. Cramer, K.O. Hogson, E.I. Stiefel and W.E. Newton, J. Am. Chem. Soc. 100 (1978) 2748;
M.S. Co, W.A. Hendrickson, K.O. Hogson and S. Doniach, J. Am. Chem. Soc. 105 (1983) 1144.
[14] C.R. Natoli and M. Benfatto, J. Phys. (Paris) 47 C-8 (1986) 11;
M. Benfatto, C.R. Natoli, A. Bianconi, J. Garcia, A. Marcelli, M. Fanfoni and Davoli, Phys. Rev. B 34 (1986) 5774;
R.F. Pettifer, D.L. Foulis and C.F.W. Hermes, J. Phys. (Paris) 47 C-8 (1986) 545.
[15] W.F. Lytle, R.B. Greefor and E.C. Marques, in: *Proc. 9th Int. Congr. on Catalysis*, eds. M.J. Phillips and M. Ternan (The Chem. Inst. Canada, Ottawa, 1988);
J.A. Horsley and R.W. Lytle, in: *Strong Metal Support Interactions*, eds. R. Baker, S. Tauster and J. Dumesic, ACS Symp. Series, Vol. 298 (Am. Chem. Soc., Washington, 1986) p. 10.
[16] M.F. Ruiz-López, M. Loos, J. Goulon, M. Benfatto and C.R. Natoli, Chem. Phys. 121 (1988) 419; *Proc. VII Int. Conf. on X-ray Absorption Fine Structure*, ed. Y. Kuroda (Japan Phys. Soc., Kobe, 1992).
[17] C.R. Natoli and M. Benfatto, J. Phys. 47 C-8 (1986) 11.
[18] J.J. Rehr, Japan. J. Appl. Phys. (1993), in press.
[19] L. Fonda, J. Phys.: Condens. Matter 4 (1992) 8269.
[20] M.F. Ruiz-López and A. Muñoz-Páez, J. Phys.: Condens. Matter 3 (1991) 8981.
[21] F.W.H. Kampers, T.M.J. Maas, J. van Grondelle, P. Brinkgreve and D.C. Koningsberger, Rev. Sci. Instr. 60 (1989) 2635.
[22] S. Hara, J. Phys. Soc. Japan 22 (1970) 710.
[23] S.H. Chou, J.J. Rehr, E.A. Stern and E.R. Davidson, Phys. Rev. B 35 (1987) 264.
[24] P. Sainctavit, J. Petiau, M. Benfatto and C.R. Natoli, Physica B 158 (1989) 347.
[25] L. Hedin and S. Lundqvist, Solid State Phys. 23 (1969) 1.
[26] M.F. Ruiz-López, A. Filipponi, A. Di Cico, T.A. Tyson, F. Bohr, M. Benfatto and C.R. Natoli, in: *X-ray Absorption Fine Structure*, ed. S.S. Hasnain (Horwood, New York, 1991) p. 75.
[27] F.M.B. Duivenvoorden, D.C. Koningsberger, Y.S. Uh and B.C. Gates, J. Am. Chem. Soc. 108 (1986) 6254.
[28] L. Bragg and G.F. Claringbull, in: *Crystal Structures of Minerals* (Bell, London, 1965).